Open access • Journal Article • DOI:10.1109/JQE.2009.2013153

Optical Feedback Self-Mixing Interferometry With a Large Feedback Factor C : Behavior Studies — Source link

Yanguang Yu, Jiangtao Xi, Joe F. Chicharo, Thierry Bosch

Institutions: University of Wollongong

Published on: 01 Jul 2009 - IEEE Journal of Quantum Electronics (IEEE)

Topics: Laser linewidth, Single-mode optical fiber, Self-mixing interferometry, Laser diode and Lasing threshold

2009

Optical feedback self-mixing interferometry with a large feedback factor C: behavior studies

Yanguang Yu
University of Wollongong, yanguang@uow.edu.au

Jiangtao Xi
University of Wollongong, jiangtao@uow.edu.au

Joe F. Chicharo
University of Wollongong, chicharo@uow.edu.au

Thierry Bosch
INPT-ENSEEIHT-LEN7, France

Optical feedback self-mixing interferometry with a large feedback factor C: behavior studies

Abstract

This paper studies the behavior of optical feedback self-mixing interferometric (OFSMI) systems, where the semiconductor lasers operate at a single mode (perturbed external cavity mode) with a large optical feedback factor *C*. Based on analysis of the spectral linewidth associated with all the possible lasing modes at different *C* values, a set of mode jumping rules are proposed following the minimum linewidth mode competition principle proposed in . According to the rules, the *C* factor can be classified into different regions, on which an OFSMI system will exhibit distinct phenomena. In particular, for the same amount of displacement associated with the external cavity, the fringe number reduction on the OFSMI signal should be observed when *C* increases from one region to the next. An experimental setup with a laser diode HL7851G was implemented and employed to verify the proposed rules. The behavior of the OFSMI predicted by the paper has been confirmed by the experiments with *C* value up to 8.0.

Disciplines

Physical Sciences and Mathematics

Publication Details

Yu, Y., Xi, J., Chicharo, J. F. & Bosch, T. (2009). Optical feedback self-mixing interferometry with a large feedback factor C: behavior studies. IEEE Journal of Quantum Electronics, 45 (7), 840-848.

Optical Feedback Self-Mixing Interferometry With a Large Feedback Factor C: Behavior Studies

Yanguang Yu, Jiangtao Xi, *Senior Member, IEEE*, Joe F. Chicharo, *Senior Member, IEEE*, and Thierry M. Bosch, *Senior Member, IEEE*

***Abstract*—This paper studies the behavior of optical feedback self-mixing interferometric (OFSMI) systems, where the semiconductor lasers operate at a single mode (perturbed external cavity mode) with a large optical feedback factor C. Based on analysis of the spectral linewidth associated with all the possible lasing modes at different C values, a set of mode jumping rules are proposed following the minimum linewidth mode competition principle proposed in [21]. According to the rules, the C factor can be classified into different regions, on which an OFSMI system will exhibit distinct phenomena. In particular, for the same amount of displacement associated with the external cavity, the fringe number reduction on the OFSMI signal should be observed when C increases from one region to the next. An experimental setup with a laser diode HL7851G was implemented and employed to verify the proposed rules. The behavior of the OFSMI predicted by the paper has been confirmed by the experiments with C value up to 8.0.**

***Index Terms*—Mode competition, optical feedback factor, optical feedback interferometry, self-mixing effect, semiconductor laser (SL).**

I. Introduction

SEMICONDUCTOR lasers (SLs) with external optical feedback has been an active area of research during the last three decades. A significant characteristic associated with an SL is the strong connection between emitted laser power (or the junction voltage) and the external optical feedback [1]–[6]. Based on this connection, a technology called optical feedback self-mixing interferometry (OFSMI) has been developed for sensing and measurement applications [7]–[18]. In contrast to other traditional interferometric techniques, OFSMI has many advantages such as simplicity in system structure, low cost in implementation, and ease in optical alignment, and hence, has attracted extensive research activities.

An OFSMI system consists of an SL packaged with photodetector (PD), a focusing lens, and a data processing unit. The PD detects the emitted power of the SL, referred to as the OFSMI signal, which is sent to the data processing unit where the signal is analyzed in order to extract useful information. The scenario behind OFSMI is a theoretical model developed from Lang and Kobayashi (L-K) equations [5], and the model is described as follows [7]–[18]:

$$\phi_F = \phi_0 - C\sin\left[\phi_F + \arctan(\alpha)\right] \tag{1}$$

$$g(\phi_0) = \cos(\phi_F) \tag{2}$$

$$P(\phi_0) = P_0\left[1 + m \times g(\phi_0)\right]. \tag{3}$$

Equation (1) gives the relationship between ϕ_0 and ϕ_F, the external light phases of an SL without and with optical feedback. These parameters are determined by $\phi_0 = 2\pi\upsilon_0\tau$ and $\phi_F = 2\pi\nu_F\tau$, respectively, where υ_0 and υ_F are the light frequencies of the SL in the two situations. τ is the external roundtrip delay determined by the external cavity length L and the speed of light c as $\tau = 2L/c$. Equation (3) gives the output power of the SL, denoted by $P(\phi_0)$, where P_0 is the power emitted by the solitude SL, m is the power modulation index, and $g(\phi_0)$ is called interference function. Obviously, when ϕ_0 varies, $g(\phi_0)$ will also vary and a modulated laser power $P(\phi_0)$ (i.e., OFSMI signal) can be observed.

There are two important parameters in the model, i.e., C and α. C is referred to as the optical feedback factor defined as follows [6], [19]–[22]:

$$C = \eta\frac{\tau}{\tau_{SL}}(1 - R_2)\sqrt{\frac{R_3}{R_2}}\sqrt{1+\alpha^2} \tag{4}$$

where R_2, R_3, η, and τ_{SL} are the power reflectivity of the laser mirrors, the power reflectivity of the external cavity surface, the coupling coefficient of the feedback power, and the round trip time in the SL chip, respectively. C is a system parameter first proposed by Lenstra *et al.* [22]. It measures the influence of optical feedback on the behavior of an SL. When $C < 1$, the situation is said to be in weak optical feedback regime, and SLs operate in a single laser cavity mode, called monostable status. When $C > 1$, the optical feedback is referred to as moderate or high regime and SLs will operate in "external cavity modes" called multistable status.

α is referred to as the linewidth enhancement factor (LEF) that is a fundamental parameter of SLs because it characterizes the SLs, such as the linewidth, the chirp, the injection lock range, and the dynamic performances. The measurement of α has been a challenging issue that has also attracted extensive research [23]–[29]. Due to the connection between the OFSMI

Manuscript received February 04, 2008; revised September 24, 2008. Current version published May 29, 2009. This work was supported by the Australian Research Council under Grant LX0561454 and by the National Natural Science Foundation of China under Grant 60574098.

Y. Yu, J. Xi, and J. F. Chicharo are with School of Electrical Computer and Telecommunications Engineering, University of Wollongong, Wollongong, N.S.W. 2522, Australia (e-mail: yanguang@uow.edu.au; yanguangyu@zzu.edu.cn; jiangtao@uow.edu.au; chicharo@uow.edu.au).

T. M. Bosch is with Institut National Polytechnique de Toulouse, Ecole Nationale Supérieure d'Electrotechnique, d'Electronique, d'Informatique, d'Hydraulique et des Télécommunications (INPT-ENSEEIHT-LEN7), Toulouse, France (e-mail: Thierry.Bosch@enseeiht.fr).

Digital Object Identifier 10.1109/JQE.2009.2013153

waveform and α, OFSMI-based approaches have been proposed for α measurement [16]–[18].

As indicated by (4), C is a parameter depending on many factors including the structure of the SL and the characteristic of the external target. As a result, it is a bit difficult to precisely control the C value in practice. In other words, OFSMI systems may operate on a wide range of C levels depending on the particular applications. Therefore, development of approaches for measuring α or retrieving movement of the external target using OFSMI in a wide range of C is an interesting and important issue.

As OFSMI technique relies on the relationship between the OFSMI signal and the parameters to be measured, the following two conditions must be met. First, a stable OFSMI signal must be observed, and second, there must be a deterministic model to describe the behavior of the OFSMI system. For the cases where $C < 1$, it is usually easy to observe a stable OFSMI signal. Also (1)–(3) are able to describe the signal waveform because (1) presents a unique mapping from ϕ_0 to ϕ_F. In this situation, the external cavity movement will result in an OFSMI signal waveform with a fringe structure similar to the traditional interference fringes, and each fringe period corresponds to 2π phase shift that is equivalent to a displacement of half wavelength of the external target [7]–[18].

When $1 < C < 4.6$, stable OFSMI signals can still be acquired for many SLs, but the behavior of the OFSMI system becomes a bit more complicated as (1) may yield three possible ϕ_F values for a particular ϕ_0, corresponding to three different lasing modes. For illustrating the situation, let us consider an example where $C = 2$ and $\alpha = 5$ and the relationships between ϕ_F and ϕ_0 as well as $g(\phi_0)$ and ϕ_0 are shown in Fig. 1. It can be seen that there are three possible modes when ϕ_0 is within $[\phi_{0,A}, \phi_{0,B}]$. According to stability analysis of lasing modes in [22], the modes are stable ones if meeting the condition $d\phi_F/d\phi_0 > 0$. In the given situation, traces $\mathrm{A_1B}$ and $\mathrm{B_1A}$ correspond to stable modes, while BA to unstable ones. The behavior of the SL has been extensively studied in this situation and it was found that although there are two stable modes in $[\phi_{0,A}, \phi_{0,B}]$, only one occurs in practice. The actual behavior is described in [10], [16], and [19], indicating that ϕ_F and $g(\phi_0)$ will vary along the path $A_1 \rightarrow B \rightarrow B_1$ when ϕ_0 increases, and they will follow the path $B_1 \rightarrow A \rightarrow A_1$ when ϕ_0 decreases. Note that points A and B are called turning points where $d\phi_F/d\phi_0 \rightarrow \infty$, as the SL exhibits a sudden mode jump when ϕ_0 approaches these two points from different directions. Obviously, hysteresis phenomenon occurs on the OFSMI signal waveforms, and the fringe shapes become sawtooth-like [10], [12], [13], [16], [19]. It should be pointed out that although the actual hysteresis behavior is well studied and well known for this situation, (1)–(3) are not able to fully describe the actual OFSMI waveform.

The challenging situation is when $C > 4.6$, in which case (1) may have more than three solutions, and hence, the SL may operate at a multistable status. As indicated by Lenstra *et al.* [22], (1) has five solutions when $4.6 < C < 7.8$, but only three solutions correspond to stable modes. When $7.8 < C < 10.9$, (1) has seven solutions, but only four correspond to stable

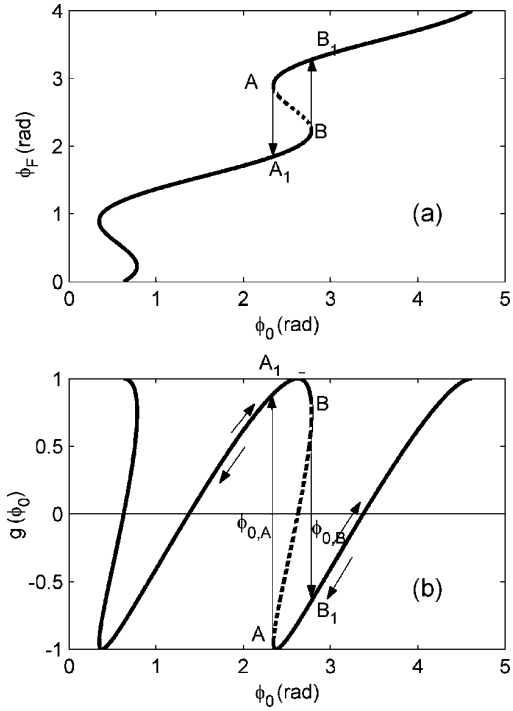

Fig. 1. Mode jump phenomenon in an OFSMI signal with $C = 2$ and $\alpha = 5$.

mode, and so on. Due to the existence of multistable modes, SLs exhibit very complicated behaviors.

In this paper, we only consider the situation where an SL operates on a single particular mode at any time, as in this case, we should be able to acquire stable OFSMI signal waveforms. In order to achieve this, we should choose the SLs with high endurance against external optical feedback. An interesting work was done by Donati *et al.* [10] reporting that a stable OFSMI signal was observed for the case of C around 6. Some OFSMI waveforms for the cases of $C > 4.6$ are also presented based on computer simulations in [15]. However, neither [10] nor [15] specify which particular mode is the one actually occurring. To identify the actual mode, we need to consider the effects of feedback on the spectra of SLs.

Regarding the spectra of SLs with feedback, five distinct feedback regimes have been identified in [20] according to the spectra characteristics. The feedback regime I corresponds to the feedback with $C < 1$, where the laser runs at a perturbed laser cavity mode. When $C > 1$, the laser runs into regimes II and III, and work at perturbed external cavity modes. At these two regimes, the mode with the minimum linewidth is the predominant lasing mode [6], [21]. So, we should able to find the actual lasing mode by comparing the linewidths for those possible lasing modes that exist in the OFSMI system.

In this paper, we will first study the linewidth characteristics for all possible stable modes at different feedback factor C, based on which a set of rules will be developed for mode jumping when SLs run into the turning points where $d\phi_F/d\phi_0 \rightarrow \infty$. These rules can be used to predict the OFSMI signal waveforms. Then we will report the experimental observations in order to confirm the theoretical analysis. The

results reported will enable us to develop novel approaches for various applications, such as the measurement of external target movement, parameter C, as well as α over a broad range of C.

II. Behavior of OFSMI With Different C Values

A. Mode Competition

When ϕ_0 is subject to a continuous change, for instance, by changing the external cavity length, ϕ_F will be forced to have a continuous change unless it reaches a turning point, over which the continuity cannot be kept and ϕ_F must jump to another stable state. Although we can exclude the unstable modes using the condition $d\phi_F/d\phi_0 > 0$ or $d\phi_0/d\phi_F > 0$, there are still more than three stable modes for the cases of $C > 4.6$. Therefore, we need to decide which particular mode is selected in practice after the jumping.

As indicated in [6] and [21] that the mode with the minimum linewidth is the predominant lasing mode, we can utilize the minimum linewidth mode competition principle to predict the behavior of an OFSMI system. In order to measure the spectral linewidth, a parameter, called the linewidth narrowing ratio (LNR), is described in [21] as follows:

$$\mathrm{LNR} = \frac{\Delta v_0}{\Delta v_F} = [1 + C\cos(\phi_F + \arctan\alpha)]^2 \tag{5}$$

where Δv_0 and Δv_F are the linewidth of an SL without and with optical feedback, respectively. Clearly, the larger the LNR, the narrower the spectral line.

For the purpose of simplicity in terms of expression, we introduce two new variables, $\Phi_F = \phi_F + \arctan(\alpha)$ and $\Phi_0 = \phi_0 + \arctan(\alpha)$, and (5) can be rewritten as

$$\mathrm{LNR} = [1 + C\cos\Phi_F]^2. \tag{6}$$

Equation (1) can also be modified as follows:

$$\Phi_F = \Phi_0 - C\sin\Phi_F. \tag{7}$$

Without loss of generality, we only consider the situation where $-\pi < \Phi_F < \pi$, as both (6) and (7) are invariant with respect to periodic extension of 2π. Considering the stable mode condition, i.e., $d\phi_F/d\phi_0 = d\Phi_F/d\Phi_0 > 0$, we have $1 + C\cos\Phi_F > 0$, and hence, $|\Phi_F| \le \arccos(-(1/C))$. Then the LNR can be expressed as

$$\mathrm{LNR} = \begin{cases} \left[1 + C\sqrt{1-\sin^2\Phi_F}\right]^2, & \text{when} \quad |\Phi_F| \le \frac{\pi}{2} \\ \left[1 - C\sqrt{1-\sin^2\Phi_F}\right]^2, & \\ \quad \text{when} \quad \frac{\pi}{2} < |\Phi_F| \le \arccos\left(-\frac{1}{C}\right). & \end{cases} \tag{8}$$

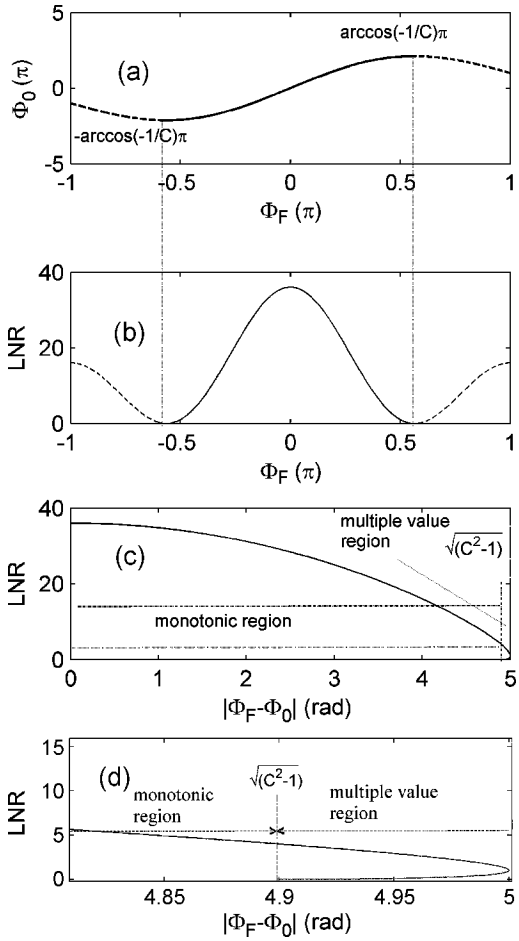

Fig. 2. Relationship between LNR and the stable modes where $C = 5$.

Also from (7), we have $C^2\sin^2\Phi_F = (\Phi_F - \Phi_0)^2 = (\phi_F - \phi_0)^2$. By substituting this relation into (8) and working out the corresponding regions for $|\Phi_F - \Phi_0|$ we have

$$\mathrm{LNR} = \begin{cases} \left[1 + \sqrt{C^2 - (\Phi_F - \Phi_0)^2}\right]^2, & \\ \quad \text{when} \quad |\Phi_F - \Phi_0| \le \sqrt{C^2-1} & \\ \left[1 \pm \sqrt{C^2 - (\Phi_F - \Phi_0)^2}\right]^2, & \\ \quad \text{when} \quad \sqrt{C^2-1} < |\Phi_F - \Phi_0| \le C. & \end{cases} \tag{9}$$

In order to illustrate the earlier analysis let us consider an example where $C = 5$. Fig. 2(a) shows the relationship between Φ_0 and Φ_F, while Fig. 2(b) presents the LNR with respect to Φ_F. Note that the segments marked by dashed lines correspond to the unstable part. Fig. 2(c) shows the LNR with respect to $|\Phi_F - \Phi_0|$ (or equivalently, $|\phi_F - \phi_0|$). Fig. 2(d) is the enlarged view for the multiple value region in Fig. 2(c), which clearly shows that the relationship has a monotonic region $|\Phi_F - \Phi_0| < \sqrt{C^2-1}$ and a multiple-value region $\sqrt{C^2-1} < |\Phi_F - \Phi_0| \le C$. In the monotonic region, the smaller the value of $|\Phi_F - \Phi_0|$, the larger the LNR, and the LNR reaches the maximum when $\Phi_F = \Phi_0$, corresponding to the narrowest linewidth. From (9), we can also see that the LNR in the monotonic region is larger than that in the multiple-value region, and that $|\Phi_F - \Phi_0|$ in monotonic region is smaller than that in the

multiple-value region. Besides, with the increase of C, the multiple-value region becomes narrower and narrower. Therefore, as long as there is one mode in the monotonic region, the mode with smallest $|\Phi_F - \Phi_B|$ is the one with the narrowest linewidth. In other words, we can find the narrowest linewidth mode simply by comparing the values of $|\phi_F - \phi_0|$.

B. Mode Jumping Rules

Now we are in the position to develop the mode jump rules for an OFSMI signal. First we should determine the turning points, where mode jumping occurs when the laser phase ϕ_0 varies in different directions. These points are characterized by $d\phi_F/d\phi_0 \to \infty$ (or equivalently, $d\Phi_F/d\Phi_0 \to \infty$) and can be determined by (1) as follows:

$$\Phi_{0,B} = 2m\pi + \varphi(C), \qquad \text{for } m = 0, 1, 2, \ldots \tag{10}$$

$$\Phi_{0,A} = 2(m+1)\pi - \varphi(C), \qquad \text{for } m = 0, 1, 2, \ldots \tag{11}$$

where $\varphi(C) = \arccos(-(1/C)) + \sqrt{C^2 - 1}$. Note that $\Phi_{0,B}$ and $\Phi_{0,A}$ corresponds to the turning points with increasing Φ_0 and decreasing Φ_0, respectively. As the $\Phi_0 \sim \Phi_F$ relationship is periodically extendable in that $(\Phi_0 + 2\pi) \sim (\Phi_F + 2\pi)$ relationship is the same as $\Phi_0 \sim \Phi_F$, these turning points also appear periodically. This is why we have integer m in (10) and (11). In the following analysis, without loss of generality, we only consider the case where $m = 0$.

Now let us consider the case when Φ_0 increases and reaches point B. The possible modes after jumping can be obtained by solving (1) with $\Phi_0 = \Phi_{0,B}$ as follows:

$$\Phi_{F,B} + C \sin \Phi_{F,B} = \varphi(C). \tag{12}$$

Obviously, the solutions of $\Phi_{F,B}$ are only determined by C, which can hence be denoted as $\Phi_{F,B_i} = \gamma(C)$.

Then we look at the value of $|\Phi_F - \Phi_0|$ for all the possible modes at the turning point B. By comparing (12) and (10), it is easy to show that $|\Phi_{F,B_i} - \Phi_{0,B}|$ are also a function of C only. In order to evaluate $|\Phi_{F,B_i} - \Phi_{0,B}|$, we carried out numerical calculations with respect to C and the results are shown in Fig. 3.

In Fig. 3, we can see several continuous curves for $|\Phi_{F,B_i} - \Phi_{0,B}|$ (where $i = 1, 2, \ldots$). With the increase of C, the first possible stable mode that the laser can jump to appears at $C = 1$. This mode is denoted as B_1, and the value of $|\Phi_F - \Phi_0|$ for this mode is shown by the curve $|\Phi_{F,B_1} - \Phi_{0,B}|$. When $C = 4.6$, the second possible mode, B_2, appears as indicated by $|\Phi_{F,B_2} - \Phi_{0,B}|$. Then the third possible mode, denoted as B_3, appears when $C = 7.8$, also shown by $|\Phi_{F,B_3} - \Phi_{0,B}|, \ldots$. In terms of the distance of the jumping in Φ_F from B, B_1 is the closest (or the next), B_2 is second next, and B_3 is the third next, and so on.

Fig. 3 also shows the variance of the monotonic region in contrast to the multiple-value region with respect to C. Fig. 3(b) is enlarged part of Fig. 3(a) in the area of $0 < C < 6.2$. It is seen that in the cases of two or more stable modes, i.e., when $C > 4.6$, there is always at least one possible mode in the monotonic region, and hence, we can simply compare the values

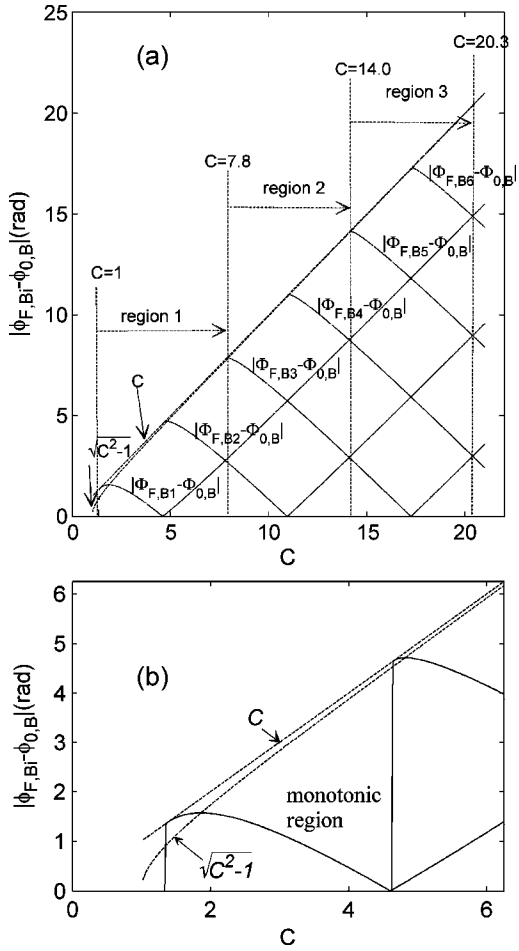

Fig. 3. $|\phi_{F,B_i} - \phi_{0,B}|$ versus C at a jumping point B. (b) Enlarged part of (a) for $0 < C < 6.2$.

of $|\Phi_{F,B_i} - \Phi_{0,B}|$ to identify which mode has the narrowest linewidth. The results in Fig. 3 enable us to divide the C value into the following regions, in which different jumping rules will apply.

1) When $1 < C < 7.8$, referred to as region 1, there are either one or two possible stable modes, denoted as B_1 and B_2, respectively. Obviously curve $|\Phi_{F,B_1} - \Phi_{0,B}|$ is either the only one (when $1 < C < 4.6$) or the lowest (when $4.6 < C < 7.8$), and hence, the mode B_1 has the minimal lindwidth and should be selected as the actual lasing mode. As B_1 appears at $C = 1$, which is the first next stable mode that laser jumps to.
2) When $7.8 < C < 14.0$, referred to as region 2, there are three or four possible stable modes, and curve $|\Phi_{F,B_2} - \Phi_{0,B}|$ is the lowest, and hence, mode B_2 will be chosen, implying that the laser will jump to the second next stable mode.
3) When $14.0 < C < 20.3$, referred to as region 3, there are five or six possible stable modes. In this case, curve $|\Phi_{F,B_3} - \Phi_{0,B}|$ is the lowest, and hence, mode B_3 will be chosen. This means laser will jump to the third next stable mode.
4) In region N, there are $2N - 1$ or $2N$ stable modes. The curve $|\Phi_{F,B_N} - \Phi_{0,B}|$ will be the lowest, and hence, mode

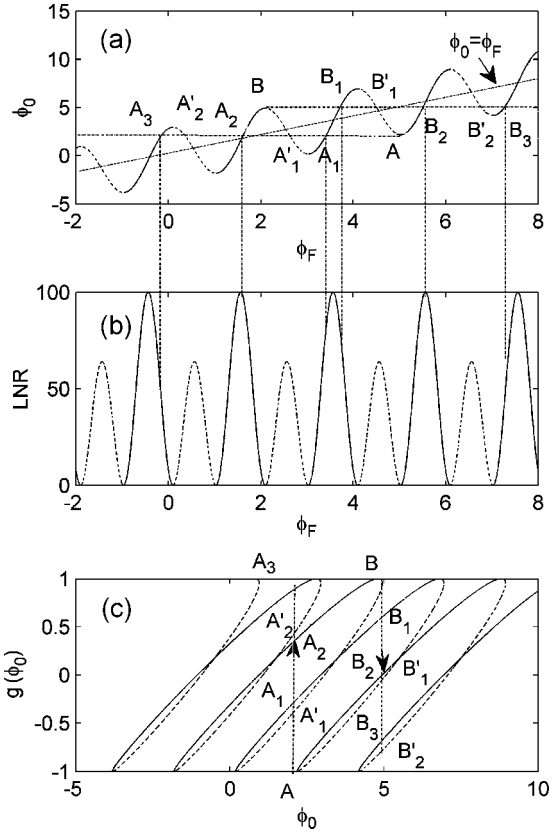

Fig. 4. Illustration of modes competition in an OFSMI signal with hgh C, where $C = 9$, $\alpha = 5$, A and B are turning points. Solid line: stable region; dotted line: unstable region. (a) ϕ_0 versus ϕ_F. (b) LNR versus ϕ_F. (c) OFSMI signal with jumps.

B_N will be chosen. Consequently, laser will jump to the Nth next stable mode.

Using the same approach described before, we are able to get similar jumping rules for the cases of decreasing ϕ_0. The laser will jump to the next stable mode when $1 < C < 7.8$ (region 1), the second next mode when $7.8 < C < 14.0$ (region 2), the third next stable mode when $14.0 < C < 20.3$ (region 3) and so on.

A special situation that should be mentioned is when the C value is at the boundaries of 7.8, 14.0, 20.3, etc. In these situations, there is one mode at the multiple-value region and also there are two possible modes with the same linewidth at the monotonic region. This particular situation will be studied in our future research.

Let us consider an example where $C = 9$ and $\alpha = 5$ in order to illustrate the earlier analysis. Fig. 4(a) shows the ϕ_0–ϕ_F relationship for this particular case. When ϕ_0 increases and ϕ_F (or $g(\phi_0)$) reaches the turning point B with its phases $(\phi_{F,B}, \phi_{0,B})$, there are five possible points (or modes) that the laser could jump to, i.e., B_1, B_1', B_2, B_2', and B_3, and among them, the stable ones are B_1, B_2, and B_3. In comparison to B_1 and B_3, we notice that B_2 has shortest distance to the diagonal line $\phi_F = \phi_0$, and hence, $|\phi_{F,B_2} - \phi_{0,B}|$ is the smallest among the three stable modes. Therefore, B_2 is characterized by minimal linewidth and will be selected as the actual lasing mode after jumping. This can also be seen in Fig. 4(b), showing that B_2 has the maximal LNR when compared to other possible modes. Similarly, when ϕ_0 decreases to reach point A $(\phi_{F,A}, \phi_{0,A})$, the laser will jump to A_2 as it has the minimal linewidth. As a result, discontinuous jumps will be observed on the OFSMI waveform. This can be seen by the ϕ_0–$g(\phi_0)$ relationship in Fig. 4(c). As B_2 is the second next mode, $g(\phi_0)$ will jump to the second next fringe.

C. Influences on OFSMI Waveforms

If the earlier jumping rules are correct, we should be able to observe an interesting phenomenon. When $g(\phi_0)$ jumps to the Nth mode, the phase difference in ϕ_0 (and also ϕ_F) between two consecutive jumps will be $2N\pi$ rather than 2π, as shown in Fig. 4(c), where $N = 2$. Accordingly, the number of fringes in the OFSMI waveform would be reduced by a factor of $1/N$ if ϕ_0 varies over the same range. Consequently, each fringe in the OFSMI waveform corresponds to a displacement of $N\lambda_0/2$ rather than the well known conclusion of $\lambda_0/2$.

In order to demonstrate the influence of the earlier jumping rules on the OFSMI waveforms, we carried out computer simulations. Without loss of generality, we assume that the external cavity is subject to a simple harmonic vibration, i.e., $L(t) = L_0 + L_1\cos(2\pi f_0 t)$, where $L_0 = 24$ cm, $L_1 = 4.2$ μm, $\lambda_0 = 785$ nm, $f_0 = 70$ Hz. The signal is sampled with the frequency of 100 kHz, and hence, we have a discrete expression for $\phi_0(t)$ as $\phi_0(n) = 3.9 \times 10^6 + 22\pi\sin(0.0044n)$. In the simulations, we assume that $\alpha = 3.5$, and C takes the values of 2, 4, 7, 8, 10, 13, 15, 17, and 19, respectively. Fig. 5 shows the simulated OFSMI waveforms. Note that the first three waveforms are all in region 1, the next three waveforms are in region 2, and the last three are in region 3. By comparing the waveforms, we are able to see the following.

1) Within each of the regions, the fringe number keeps almost unchanged, but the swinging of fringes decreases when increasing C.
2) Fringe number reduction will occur when C varies over different regions. Supposing the number of fringes is M in region 1, the number of fringes reduced to $M/2$ in region 2, $M/3$ in region 3, and so on.
3) When C varies across the boundaries, we should observe a sudden increase in the swinging of fringes.

III. Experiment and Discussion

In order to test the jumping rules developed before, we implemented an experimental OFSMI system, shown in Fig. 6. The optical setup consists of a laser diode (LD), a focus lens, and a loudspeaker as the external target. The electrical setup consists of LD driving devices, an optical power detection circuit, and a digital oscilloscope. In the experiment, the LD is HL7851G with wavelength of $\lambda_0 = 785$ nm and the LD is biased with a dc current of 90 mA and operates at single mode. We choose this LD because it has high endurance against external optical feedback, i.e., the SL can operate in a single mode at a high C level. The sinusoidal signal driving the loudspeaker is 73 Hz and has peak-to-peak (p-p) amplitude of 736 mV. The temperature of LD is maintained at 25 ± 0.1 °C by means of a temperature controller. The earlier experiment conditions are kept unchanged throughout the experiment. As indicated by (4), C is

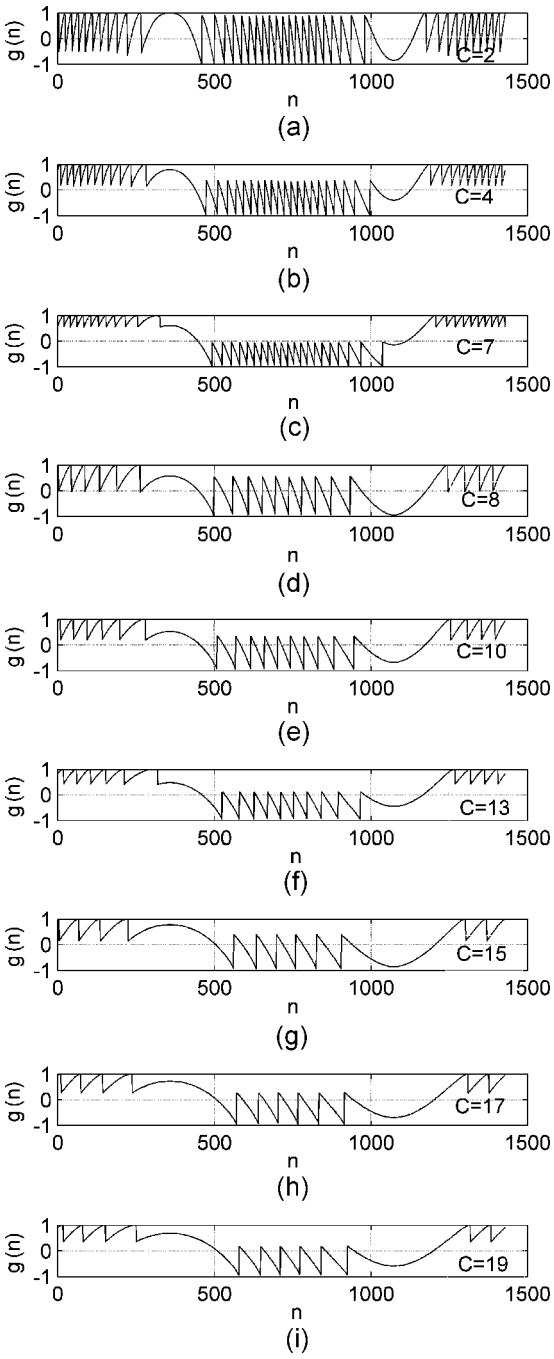

Fig. 5. Simulated OFSMI waveforms with $\alpha = 3.5$ at different regions for same ϕ_0.

proportional to τ, the round trip time of the external cavity given by $\tau = 2L_0/c$, and hence, different C values can be realized by varying the external cavity length L_0.

With the setup we have acquired various OFSMI waveforms following the procedures given shortly and Fig. 7 shows some of the waveforms copied from the digital oscilloscope. Also we normalized the raw waveforms by removing the dc component and noises shown in Fig. 8 for evaluating the C value.

We start from placing external target about 10 cm away from the laser and a stable OFSMI waveform was obtained. Then we gradually increase the distance until 70 cm, and we found that

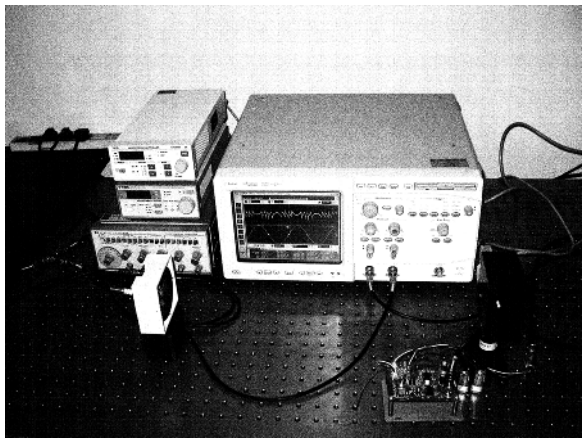

Fig. 6. OFSMI experimental setup.

stable waveforms can always be obtained. Fig. 8(a)–(f) shows the waveforms for L_0 being around 10, 30, 40, 50, 60, and 70 cm, respectively. In order to determine C levels, we have also done computer simulations.

By comparing the experimental waveforms in Fig. 8 with the simulations, we found that the C values are about 1.35, 3.30, 5.57, 6.00, 6.80, and 7.40 respectively. We noticed that the number of fringes is almost the same, and the swinging of the fringes decreases with the C level. This is consistent with what is expected by the conclusion in Section II-C as the SL operates in region 1 for these cases. Although there is a slight difference between the waveforms in Fig. 8 in terms of the fringe numbers, we believe that it is caused by the differences in the vibration amplitude of the loudspeaker, as both the speaker and the driving signals are not ideal. Also note that each fringe corresponds to a displacement of half wavelength.

When L_0 is around 80 cm, we captured an interesting phenomenon, which is shown in Fig. 9. In order to understand the phenomenon, we recorded the sinusoid driving signal used for the loudspeaker and the corresponding OFSMI signal at the same time. It can be seen that the OFSMI waveforms exhibit different fringe structures during the two different half vibration cycles. For the half cycle when the target moves away from the LD, the fringe number is closed to the cases in Fig. 8(f), but the fringe number reduces to half for the other half cycle when the target moves toward the LD. This is an interesting phenomenon as it implies that C levels are different with respect to these two half cycles. In order to explain this, we carried out simulations of OFSMI waveforms with different C levels, and then compare them with the waveform in Fig. 9. After trying different C values, we found that the first half in Fig. 9 is very similar to a segment of the simulated waveform where C is slightly smaller than the boundary 7.8, and the second half in Fig. 9 is similar to these where C is slightly larger than 7.8. The simulations are shown in Fig. 10, where Fig. 10(a) shows the variation of $\phi_0(n)$, and Figs. 10(b) and (c) are the OFSMI waveforms for C with 7.6 and 8.0 respectively. With a careful observation on the waveform in Fig. 9, we found a transition moment T (see Fig. 10). By combining the section before T in Fig. 10(b) and the section after T in Fig. 10(c), we obtain a waveform in Fig. 10(d) that is very similar to the experimental observation shown in Fig. 9.

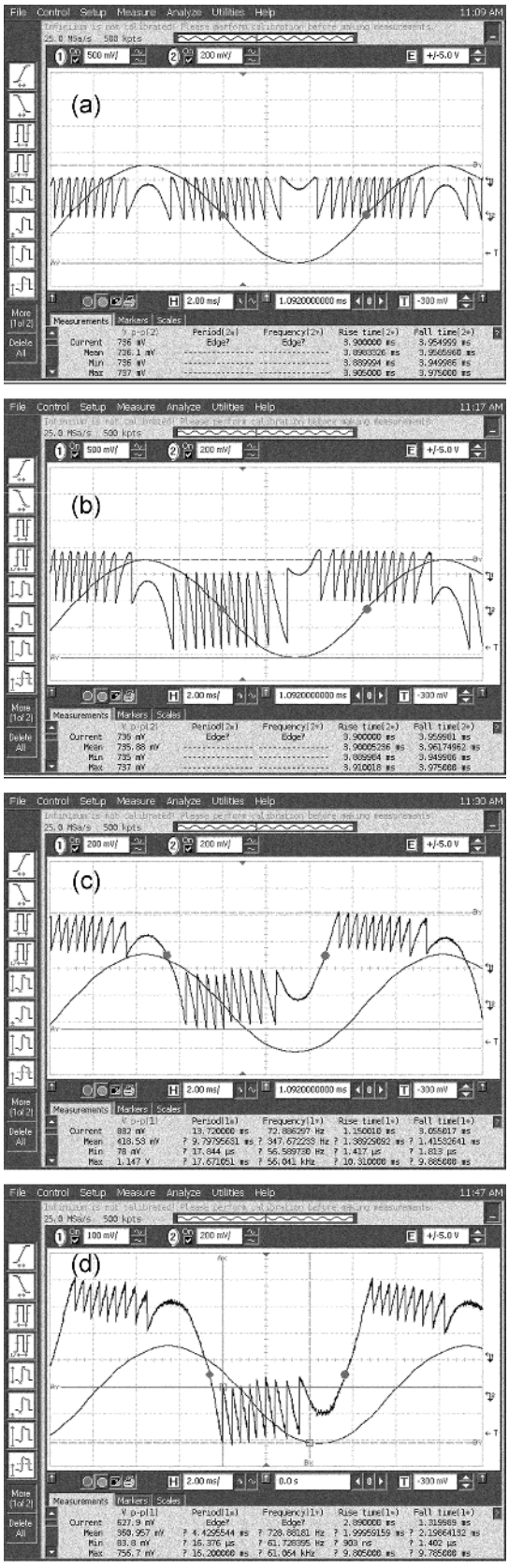

Fig. 7. Experimental OFSMI signal waveform displayed on the oscilloscope.

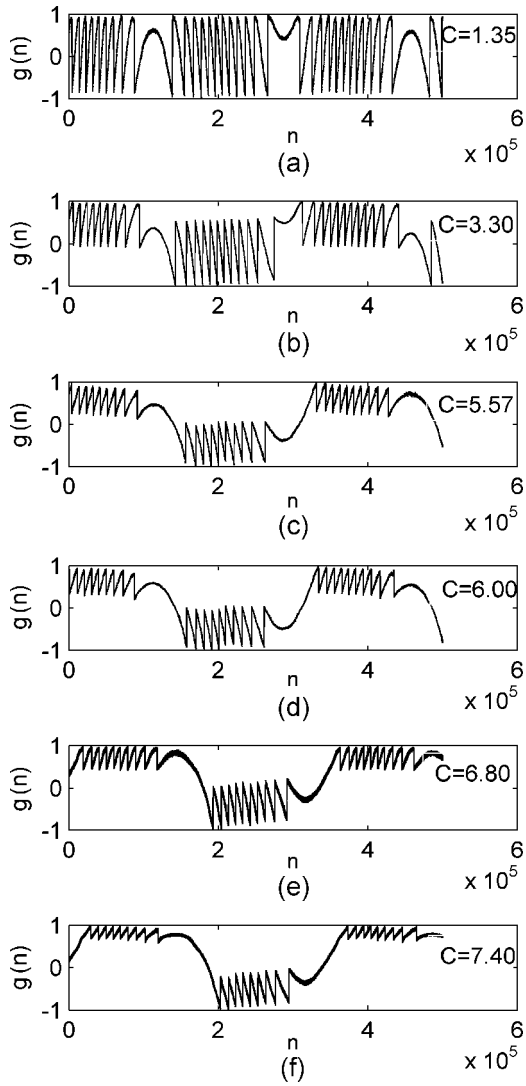

Fig. 8. Normalized experimental signals with different C values.

Therefore, we can say that C varied from region 1 to region 2 at the point T in Fig. 9. People may argue that the vibration amplitude is much smaller than the external cavity length, and so there is no big change in C during a vibration cycle. However, as indicated by (4), the C value also depends on other factors, such as coupling coefficient η. The movement of the external target during the two half vibration cycles may not be exactly symmetrical, which may result in a change of η. As a result, there may be a slight variance in C when external target moves in two opposite directions. This slight variance, when spanning the point of $C = 7.8$, will result in the waveform shown in Fig. 10(d).

We also tried to achieve higher C level by increasing L_0. However, when L_0 are over 80 cm, the observed waveforms become unstable. In other words, with the existing experimental system and the LD, we were not able to obtain stable waveforms with C value at region 2 for a full vibration cycle of the loudspeaker. In region 2 or higher regions, there exist more than seven possible modes, and increasing the external cavity length will make the mode very closely spaced. As a result, the SL may operate on multiple modes, which is out of the scope of this paper.

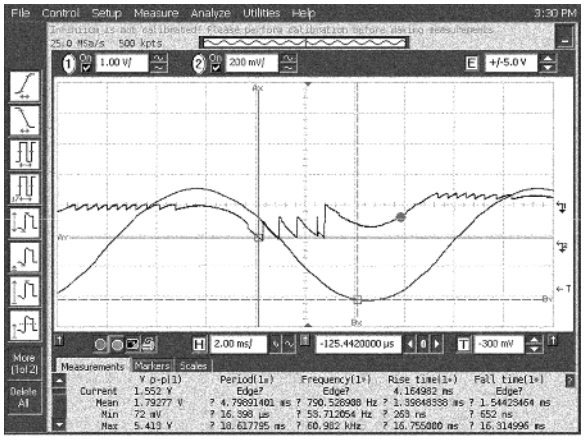

Fig. 9. Phenomenon of fringe reduction recorded by oscilloscope.

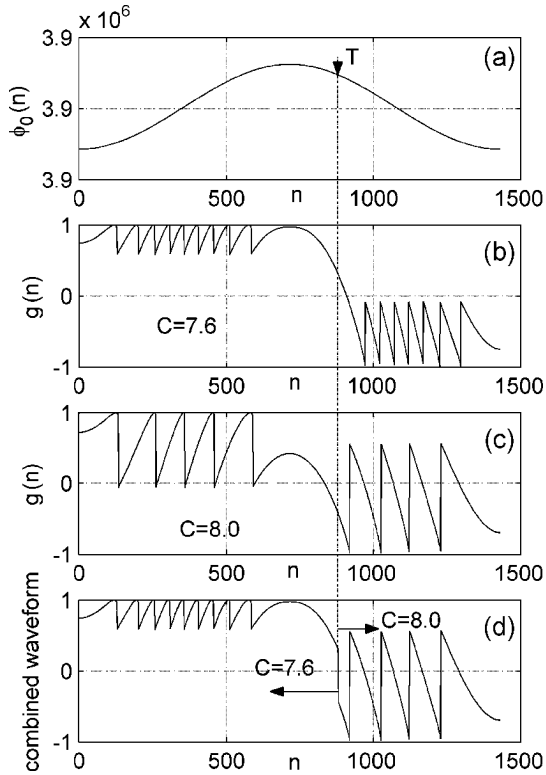

Fig. 10. Illustration for the fringe reduction observed in Fig. 9, where T is set as the transition moment.

IV. Conclusion

This paper studies the behavior of an OFSMI system containing a single-mode (perturbed external mode) SL, which operates with different optical feedback factor C. Based on the analysis of the spectral linewidth associated with all the possible stable modes, we developed a set of rules for determining the mode when the SL runs into the turning points (where $(d\phi_F/d\phi_0) \rightarrow \infty$) due to the change of external feedback phase. Based on these rules, the feedback factor C can be classified into the following distinct regions, in which the OFSMI will exhibit different behavior. The case of $1 < C < 7.8$ is referred to as region 1, $7.8 < C < 14.0$ as region 2, $14.0 < C < 20.3$ as region 3, etc. When the SL operates in region 1 and runs over a turning point, it will jump to the next stable mode. The SL will jump to the second next stable mode if operating in region 2, and similarly it will jump to the third next stable mode when operating in region 3. As a result of the mode jumping described, reduction of fringe number on OFSMI waveforms should be observed. In region 1, the number of fringes is still $M = 2L_1/\lambda_0$ for a given displacement of external target L_1, but for the same displacement, the fringe number will reduce to $M/2$ if the SL operates in region 2, and the fringe number will be $M/3$ in region 3, etc.

The behavior described before has been verified using an experimental OFSMI system with an LD HL7851G at the range of $1 < C < 8.0$.

The presented results provide novel models for the OFSMI systems especially for the cases of $C > 4.6$. With these new models, novel OFSMI-based techniques can be developed for many potential applications. For example, displacement can be measured when $C > 4.6$. In these cases, the resolution for displacement measurement using simple fringe counting on OFSMI signals is $N\lambda_0/2$ (when the SL operates in region N), which is different from the well-known conclusion of $\lambda_0/2$. Also measurement of the α over a large range of C may help to reveal the relationship between the α and C of the SL systems.

Acknowledgment

The authors would like to thank Y. Zhao, Zhengzhou University, China, for his assistance in the experimental work.

References

[1] A. P. Bogatov, P. G. Eliseev, L. P. Ivanov, A. S. Logginov, M. A. Manko, and K. Y. Senatorov, "Study of the single-mode injection laser," *IEEE J. Quantum Electron.*, vol. QE-9, no. 2, pp. 392–398, Feb. 1973.

[2] C. Voumard, R. Salathe, and H. Weber, "Resonance amplifier model describing diode lasers coupled to short external resonators," *Appl. Phys.*, vol. 12, pp. 369–378, Apr. 1977.

[3] K. Kobayashi, "Improvements in direct pulse code modulation of semiconductor lasers by optical feedback," *Trans. IEICE Japan*, vol. E59, no. 12, pp. 8–14, Dec. 1976.

[4] Y. Mitsuhashi, T. Morikawa, K. Sakurai, A. Seko, and J. Shimada, "Self-coupled optical pickup," *Opt. Commun.*, vol. 17, pp. 95–97, Apr. 1976.

[5] R. Lang and K. Kobayashi, "External optical feedback effects on semiconductor injection laser properties," *IEEE J. Quantum Electron.*, vol. QE-16, no. 3, pp. 347–355, Mar. 1980.

[6] K. Petermann, "External optical feedback phenomena in semiconductor lasers," *IEEE J. Sel. Topics Quantum Electron.*, vol. 1, no. 2, pp. 480–489, Jun. 1995.

[7] S. Shinohara, A. Mochizuki, H. Yoshida, and M. Sumi, "Laser Doppler velocimeter using the self-mixing effect of a semiconductor laser diode," *Appl. Opt.*, vol. 25, no. 9, pp. 1417–1419, 1986.

[8] P. J. de Groot, G. M. Gallatin, and S. H. Macomber, "Ranging and velocimetry signal generation in a backscatter-modulated laser diode," *Appl. Opt.*, vol. 27, no. 21, pp. 4475–4480, Nov. 1988.

[9] W. M. Wang, K. T. V. Grattan, A. W. Palmer, and W. J. 0. Boyle, "Self-mixing interference inside a single-mode diode laser for optical sensing applications," *J. Lightw. Technol.*, vol. 12, no. 9, pp. 1577–1587, Sep. 1994.

[10] S. Donati, G. Giuliani, and S. Merlo, "Laser diode feedback interferometer for measurement of displacements without ambiguity," *IEEE J. Quantum Electron.*, vol. 31, no. 1, pp. 113–119, Jan. 1995.

[11] J. Kato, N. Kikuchi, I. Yamaguchi, and S. Ozono, "Optical feedback displacement sensor using a laser diode and its performance improvement," *Meas. Sci. Technol.*, vol. 6, pp. 45–52, Jan. 1995.

[12] N. Servagent, F. Gouaux, and T. Bosch, "Measurements of displacement using the self-mixing interference in a laser diode," *J. Opt.*, vol. 29, no. 3, pp. 168–173, Jun. 1998.

[13] G. Giuliani, M. Norgia, S. Donati, and T. Bosch, "Laser diode self-mixing technique for sensing applications," *J. Opt. A: Pure Appl. Opt.*, vol. 4, pp. S283–S294, 2002.
[14] L. Scalise, Y. Yu, G. Giuliani, G. Plantier, and T. Bosch, "Self-mixing laser diode velocimetry: Application to vibration and velocity measurement," *IEEE Trans. Instrum. Meas.*, vol. 53, no. 1, pp. 223–232, Feb. 2004.
[15] G. Plantier, C. Bes, and T. Bosch, "Behavior model of a self-mixing laser diode sensor," *IEEE J. Quantum Electron.*, vol. 41, no. 9, pp. 1157–1167, Sep. 2005.
[16] Y. Yu, G. Giuliani, and S. Donati, "Measurement of the linewidth enhancement factor of semiconductor lasers based on the optical feedback self-mixing effect," *IEEE Photon. Technol. Lett.*, vol. 16, no. 4, pp. 990–992, Apr. 2004.
[17] J. Xi, Y. Yu, J. Chicharo, and T. Bosch, "Estimating the parameters of semiconductor lasers based on weak optical feedback interferometry," *IEEE J. Quantum Electron.*, vol. 41, no. 8, pp. 1058–1064, Aug. 2005.
[18] Y. Yu, J. Xi, J. Chicharo, and T. Bosch, "Toward automatic measurement of the linewidth enhancement factor using optical feedback self-mixing interferometry with weak optical feedback," *IEEE J. Quantum Electron.*, vol. 43, no. 7, pp. 527–534, Jul. 2007.
[19] G. A. Acket, D. Lenstra, A. J. D. Boef, and B. H. Verbeek, "The influence of feedback intensity on longitudinal mode properties and optical noise in index-guided semiconductor lasers," *IEEE J. Quantum Electron.*, vol. QE-20, no. 10, pp. 1163–1169, Oct. 1984.
[20] R. W. Tkach and A. R. Chraplyry, "Regime of feedback effects in 1.5 um, DFB lasers," *J. Lightw. Technol.*, vol. 14, no. 11, pp. 1655–1611, Nov. 1986.
[21] N. Schunk and K. Petermann, "Numerical analysis of the feedback regimes for a single-mode semiconductor laser with external feedback," *IEEE J. Quantum Electron.*, vol. 24, no. 7, pp. 1242–1247, Jul. 1988.
[22] D. Lenstra, M. van Vaalen, and B. Jaskorzynska, "On the theory of a single-mode laser with weak optical feedback," *Physica*, vol. 125C, pp. 255–264, 1984.
[23] M. Osinski and J. Buus, "Linewidth broadening factor in semiconductor lasers—An overview," *IEEE J. Quantum Electron.*, vol. QE-23, no. 1, pp. 9–28, Jan. 1987.
[24] G. Liu, X. Jin, and S. L. Chuang, "Measurement of linewidth enhancement factor of semiconductor lasers using an injection-locking technique," *IEEE Photon. Technol. Lett.*, vol. 13, no. 5, pp. 430–432, May 2001.
[25] L. Shterengas, G. L. Belenky, and A. Gourevitch, "Measurerments of a-factor in 2–2.5 um type-I In(Al)GaAsSb/GaSb high power diode lasers," *Appl. Phys. Lett.*, vol. 81, pp. 4517–4519, Dec. 2002.
[26] T. B. Simpson, F. Doft, E. Strzelecka, W. Chang, and G. J. Simonis, "Gain saturation and the linewidth enhancement factor of semiconductor lasers," *IEEE Photon. Technol. Lett.*, vol. 13, no. 8, pp. 776–778, Aug. 2001.
[27] A. Hsu, J. F. P. Seurin, S. L. Chuang, and K. D. Choquette., "Optical feedback in vertical-cavity surface-emitting lasers," *IEEE J. Quantum Electron.*, vol. 37, no. 12, pp. 1643–1649, Dec. 2001.
[28] H. Halbritter, F. Riemenschneider, J. Jacquet, J. G. Provost, C. Symonds, I. Sagnes, and P. Meissner, "Chirp and linewidth enhancement factor of tunable, optically-pumped long wavelength VCSEL," *Electron. Lett.*, vol. 40, no. 4, pp. 242–244, Feb. 2004.
[29] P. K. Kondratko, S. L. Chung, and N. Holonyak, "Observations of near-zero linewidth enhancement factor in a quantum-well coupled quantum-dot laser," *Appl. Phys. Lett.*, vol. 83, no. 6, pp. 4818–4820, Dec. 2003.

Yanguang Yu received the B.E. degree from Huazhong University of Science and Technology, Wuhan, China, in 1986 and the Ph.D. degree from Harbin Institute of Technology, Harbin, China, in 2000, both in electrical engineering.

She was with the College of Information Engineering, Zhengzhou University, China, where she was a Lecturer (1986–1999), an Associate Professor (2000–2004), and a Professor (2005–2007). During 2001 and 2002, she was a Postdoctoral Fellow with the Opto-Electronics Information Science and Technology Laboratory, Tianjin University, China. She was also a Visiting Fellow with the Optoelectronics Group, Department of Electronics, University of Pavia, Italy (2002–2003), and a Visiting Associate Professor and a Professor with the Engineering School (ENSEEIHT) of Toulouse, France, respectively, in 2004 and 2006. She is currently a Research Fellow with the Information and Communication Technology Research Institute (ICTR), University of Wollongong, Wollongong, N.S.W., Australia, where she was also a Principal Visiting Fellow during 2004–2005. Her current research interests include semiconductor lasers with optical feedback and optical feedback interferometry and their applications to instrumentation and measurement.

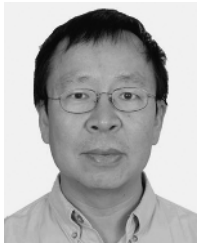

Jiangtao Xi (S'93–M'95–SM'06) was born in China in 1962. He received the B.E. degree from Beijing Institute of Technology, Beijing, China, in 1982, the M.E. degree from TsingHua University, Beijing, in 1985, and the Ph.D degree from the University of Wollongong, Wollongong, N.S.W., Australia, in 1996, all in electrical engineering.

From 1995 to 1996, he was a Postdoctoral Fellow with the Communications Research Laboratory, McMaster University, ON, Canada. From 1996 to 1998, he was a Member of the Technical Staff with Bell Laboratories, Lucent Technologies, Inc. From 2000 to 2002, he was the Chief Technical Officer with TCL IT Group Company, China. In 2003, he joined the University of Wollongong as a Senior Lecturer and is currently an Associate Professor. His current research interests include signal processing and its applications in various areas, including telecommunications, speech and audio processing, as well as optoelectronic systems.

Joe F. Chicharo (S'86-M'90–SM'96) received the Bachelor's degree (with first-class honors) and the Ph.D. degree from the University of Wollongong, Wollongong, N.S.W., Australia, in 1983 and 1990, respectively, both in electrical engineering.

Since 1985, he has been with the University of Wollongong, where he was a Lecturer (1985–1990), a Senior Lecturer (1990–1994), and an Associate Professor (1994–1997), has been a Professor since 1997, was the Dean of the Faculty of Informatics (2003–2008), and is the Pro Vice-Chancellor (International). His current research interests include the areas of signal processing, telecommunications, and information technology. He has authored or coauthored more than 200 research publications.

Prof. Chicharo was the Research Director of the Australian Collaborative Research Center on Smart Internet Technology from 2000 to 2003. From 2005 to 2007, he was the Chair of the Australian Research Council, Mathematics and Information Communications Sciences panel. He is the President of the Australian Council of Deans of Information, Communications and Technology.

Thierry M. Bosch (M'93–SM'06) received the M.S. and Ph.D. degrees from the National Institute of Science of Toulouse (INSAT), Toulouse, France, in 1989 and 1992, respectively.

He is a Research Coordinator of the Engineering School ENSEEIHT and the Director of the Laboratory of Optoelectronics for Embedded Systems in Toulouse. His current research interests include laser industrial instrumentation development, including range finding techniques, vibration and velocity measurements. He has cooperated in several programs of R&D with European companies active in the areas of sensor design, metrology, transportation, or avionics. He has coauthored more than 35 papers published in archival journals. He has also been invited to author the chapter dedicated to the optical feedback interferometry published in the *Encyclopedia of Sensors (2006)*. He has coedited the Milestone Volume entitled *Selected Papers on Laser Distance Measurements* (SPIE, 1995).

Prof. Bosch is the Chairman of the IEEE Instrumentation and Measurement Technical Committee "Laser & Optical Systems" and is an Associate Editor of the IEEE TRANSACTIONS ON INSTRUMENTATION AND MEASUREMENT and the International Journal on Smart Sensing and Intelligent Systems.